Correlation between Magnetic Properties and Mn/Co Atomic Order in $LaMn_{0.5}Co_{0.5}O_{3+\delta}$: I. Second-Order Nature in Mn/Co Atomic Ordering and Valence State

Tôru Kyômen, Ryutaro Yamazaki, and Mitsuru Itoh*

Materials and Structures Laboratory, Tokyo Institute of Technology, 4259 Nagatsuta, Midori-ku, Yokohama 226-8503, Japan

Received May 27, 2003. Revised Manuscript Received October 1, 2003

The relaxation phenomenon around 1300 K in $LaMn_{0.5}Co_{0.5}O_{3+\delta}$ and their valence states of Mn and Co atoms were investigated by TG-DTA, powder X-ray diffraction, magnetic susceptibility, and XANES of two samples cooled at 10 Kh^{-1} in the range 1673−973 K and quenched from 1673 K. DTA clarified that the relaxation phenomenon is not due to a first-order phase transition and that the temperature dependence of relaxation time is a thermal activation type, which suggests that the order−disorder phase transition of Mn/Co atomic ordering is second-order type. The results of lattice parameters, XANES, and magnetic susceptibility measurements suggest that the ground valence state of the ordered phase is Mn^{4+}/Co^{2+} and that a fraction of Mn^{3+}/Co^{3+} is increased either by disordering the Mn/Co atomic configuration or by increasing temperature.

Introduction

Disorder in magnetic interactions originating from disorder in atomic configuration in a material often induces spin-glass, cluster glass, or mictomagnetic behaviors as a macroscopic magnetism. It is usually difficult to suppose the detail of atomic scale disorder from the macroscopic properties. It is thus useful to investigate the change of magnetic properties in a material by controlling the atomic order. A perovskite-type oxide $LaMn_{0.5}Co_{0.5}O_3$ is expected to be an appropriate material for this purpose, because the control of Mn/Co atomic order would be possible according to earlier studies described below.

The ferromagnetic behavior in $LaMn_{1-x}Co_xO_3$ has been first reported by Goodenough et al.[1] Their original idea is that the ferromagnetism originates from Mn^{3+}−Mn^{3+} vibronic superexchange interaction.[1,2] Blasse concluded from the Curie constant of $LaMn_{0.5}Co_{0.5}O_3$ that Mn and Co atoms are in tetravalent and divalent states, respectively.[3] He suggested that Mn^{4+} and Co^{2+} ions are arranged in a rocksalt-type structure and that the Mn^{4+}−Co^{2+} superexchange interaction is the origin of ferromagnetism. Jonker also concluded from the resistivity and Seebeck coefficient that neighbor pairs of Mn and Co atoms transform into Mn^{4+} and Co^{2+} and from the Curie constant that the fraction of Mn^{3+}/Co^{3+} (high spin) in $LaMn_{0.5}Co_{0.5}O_3$ increases as the order parameter of Mn/Co atomic configuration decreases.[4] He mentioned that at least three exchange interactions, Mn^{3+}−Mn^{3+}, Mn^{4+}−Mn^{3+}, and Mn^{4+}−Co^{2+}, are positive.[4] The ^{55}Mn NMR study of $La(Co_{1-x}Mg_x)_{0.5}Mn_{0.5}O_3$ clearly demonstrated a presence of Mn^{4+} ions and the ordered configuration of Mn^{4+} and Co^{2+} ions.[5,6] Recently, Bull et al. reported the long-range order of Mn/Co atomic configuration in $LaMn_{0.5}Co_{0.5}O_3$ by neutron diffraction measurements and suggested that the space group at room temperature is $P2_1/n$ with the Mn/Co atomic configuration of rocksalt-type.[7,8] It is found from these studies that the valence states of Mn/Co ions and their configurations are important to understanding the magnetic interaction in $LaMn_{0.5}Co_{0.5}O_3$.

The earlier studies have reported that the magnetic properties of $LaMn_{0.5}Co_{0.5}O_3$ are changed by cooling rate around 1300 K.[3−6] They concluded that the Mn/Co atomic ordering freezes-in below about 1300 K. Figure 1 shows this situation. The order parameter increases with decreasing temperature. Because the relaxation time of ordering enlarges with decreasing temperature, the order parameter freezes-in at a nonequilibrium value. Thus, the frozen order parameter depends on the cooling rate. The lower order parameter would induce a spin-glass-like behavior at low temperatures. However, there is no detailed information on the relaxation phenomenon, such as relaxation time, for $LaMn_{0.5}Co_{0.5}O_3$.

The first purpose of the present study is to investigate the relaxation phenomenon in detail in order to under-

* To whom correspondence should be addressed. Phone and Fax: 81-45-924-5354. E-mail: mitsuru_itoh@msl.titech.ac.jp.

(1) Goodenough, J. B.; Wold, A.; Arnott, R. J.; Menyuk, N. *Phys. Rev. B* **1961**, *124*, 373.
(2) Zhou, J.-S.; Yin, H. Q.; Goodenough, J. B. *Phys. Rev. B* **2001**, *63*, 184423.
(3) Blasse, G. *J. Phys. Chem. Solids* **1965**, *26*, 1969.
(4) Jonker, G. H. *J. Appl. Phys.* **1966**, *37*, 1424.
(5) Nishimori, N.; Asai, K.; Mizoguchi, M. *J. Phys. Soc. Jpn.* **1995**, *64*, 1326.
(6) Asai K.; Fujiyoshi, K.; Nishimori, N.; Satoh, Y.; Kobayashi, Y.; Mizoguchi, M. *J. Phys. Soc. Jpn.* **1998**, *67*, 4218.
(7) Bull, C. L.; Motimer, R.; Sankar, G.; Gleeson, D.; Catlow, C. R. A.; Wood, I. G.; Price, G. D. *Synth. Met.* **2001**, *121*, 1467.
(8) Bull, C. L.; Gleeson, D.; Knight, K. S. *J. Phys.: Condens. Matter* **2003**, *15*, 4927.

10.1021/cm0302781 CCC: $25.00
Published on Web 11/08/2003

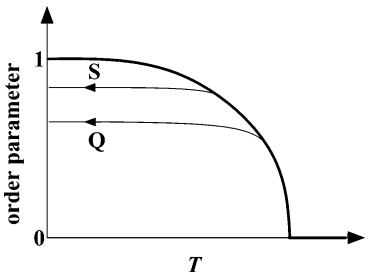

Figure 1. Predicted temperature dependence of long-range order parameter with respect to the Mn/Co atomic configuration in $LaMn_{0.5}Co_{0.5}O_3$. A thick line represents the equilibrium curve. Thin lines indicated by S and Q represent the curves expected for the sample to follow on cooling when the sample was cooled slowly and quenched, respectively.

stand the nature of Mn/Co atomic ordering and how to control the order parameter by thermal treatments. Particularly, it should be clarified whether the long-range ordering occurs through a first-order or a second-order phase transition, because two-phase coexistence has been reported so far in cooling-rate controlled samples.[9] The present results show that the phase transition is second-order type similar to a usual order−disorder phase transition in alloy. It is found that the temperature dependence of relaxation time is a thermal activation type as expected from earlier studies.[3−6] Here, the orthorhombic-to-rhombohedral phase transition reported by Bull et al.[7] is useful in order to investigate the relaxation phenomenon. Thus, the structural phase transition is also reported in this paper. The second purpose of this study is to clarify the valence state of Mn/Co ions in the whole temperature region and their relation to the Mn/Co atomic order. The present result is consistent with Jonker's suggestion that the fraction of Mn^{3+}/Co^{3+} ions increases with decreasing the Mn/Co atomic order. In addition, the present study suggests that the thermal equilibrium reaction occurs with the activation energy of the order of 1000 K between Mn^{4+}/Co^{2+} and Mn^{3+}/Co^{3+} states even in the well-ordered sample. The magnetic properties at low temperatures will be reported in a forthcoming Part II paper.[10]

Experimental Section

The $LaMn_{0.5}Co_{0.5}O_{3+\delta}$ polycrystalline sample was prepared by a solid-state reaction method. Appropriate amounts of La_2O_3, MnO_2, and $CoC_2O_4{\cdot}2H_2O$ were mixed in an agate mortar with ethanol and calcined in air at 1273−1573 K with some intermittent grindings. The calcined powder was pressed into pellets and sintered in air at 1673 K for 24 h. One pellet was quenched into air at room temperature from 1673 K, and another was cooled from 1673 to 973 K at 10 Kh^{-1} and then down to room temperature in a furnace. The former and latter samples are referred to as quenched and slowly cooled samples, respectively, in this paper. Iodometric titration determined the excess oxygen compositions, δ, of the slowly cooled and quenched samples to be 0.04 ± 0.02 and 0.03 ± 0.02, respectively. For the references of XANES measurements, $LaCoO_3$ and $LaMnO_3$ were prepared by a solid-state reaction method in air and Ar atmosphere, respectively. Commercial CoO, MnO, and MnO_2 were also used for the reference of XANES measurements.

(9) Dass, R. I.; Goodenough J. B. *Phys. Rev. B* **2003**, *67*, 014401.
(10) Kyômen, T.; Yamazaki, R.; Itoh, M. *Chem. Mater.* submitted for publication.

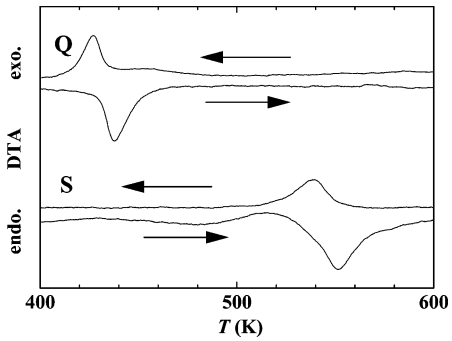

Figure 2. DTA curves on heating and cooling processes at a rate 10 $Kmin^{-1}$: Q, quenched sample; S, slowly cooled sample.

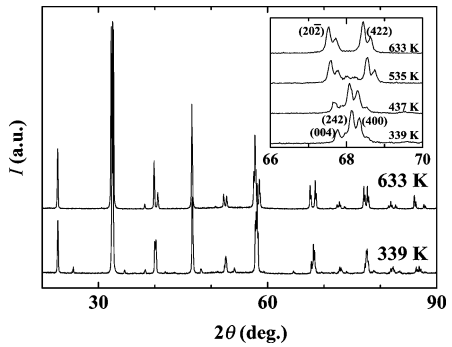

Figure 3. Powder XRD patterns of slowly cooled sample at 339 and 633 K. Inset shows the temperature dependence of XRD patterns in the range $2\theta = 66-70°$ on an enlarged scale.

Powder X-ray diffraction measurements were carried out using Cu Kα radiation (MAC Science, MXP18HF). Lattice parameters were determined in a range 30−830 K from some diffraction peaks in a high 2θ region using Si crystalline powder as an internal standard. The XRD pattern and lattice parameters at room temperature did not change before and after the sample was heated to 830 K. This indicates neither appreciable oxidation of Si nor chemical reaction between Si and the sample up to 830 K at least during the measurement period. TG-DTA was carried out in air in a range 373−1573 K (MAC Science, 2000S). Because neither appreciable mass gain nor reduction was observed within the experimental error in the measurement temperature range, only the results of DTA are reported in this paper. Magnetic susceptibilities were measured in a range 5−300 K under 50 Oe using a SQUID magnetometer (Quantum Design, MPMS5S) and in a range 300−1100 K using a magnetic balance (Simadzu, MB-1A). Mn-*K* edge and Co-*K* edge XANES were measured at room temperature using Mo radiation (RIGAKU, R-XAS Looper).

Results

Orthorhombic-to-Rhombohedral Phase Transition. Figure 2 shows the DTA curves on heating and cooling processes for the quenched (indicated by Q) and slowly cooled (indicated by S) samples. An exothermic and an endothermic phenomena were observed on heating and cooling processes, respectively, in each sample, corresponding to the orthorhombic-to-rhombohedral phase transition as reported by Bull et al.[7] The exothermic and endothermic peak temperatures are different from each other in the same sample, which indicates a first-order nature of phase transition. The transition temperature of slowly cooled sample is higher than that of the quenched sample.

Figure 3 shows the powder XRD patterns of slowly cooled sample at 339 and 633 K. It was found that the

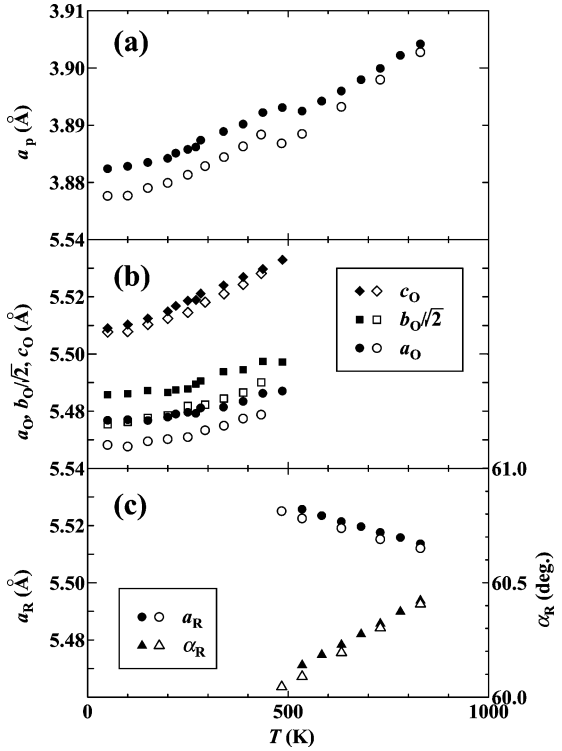

Figure 4. Temperature dependence of (a) a_p (see text), (b) lattice parameters of the low-temperature orthorhombic phase, and (c) lattice parameters of the high-temperature rhombohedral phase. Solid and open symbols indicate the values of slowly cooled and quenched samples, respectively.

structural phase transition occurs between 339 and 633 K. The XRD patterns at 339 and 633 K were indexed by an orthorhombic unit cell and a rhombohedral one, respectively. It was impossible to judge whether the symmetry is lower than *Pnma* or $R\bar{3}c$, because no appreciable superlattice reflection indicating the Mn/Co atomic order could be detected. This is not in contradiction with Bull's report that the space group is $P2_1/n$ at room temperature, because they also detected no superlattice reflection by X-ray diffraction despite the observation by the neutron diffraction.[7] The inset of Figure 3 shows the temperature dependence of XRD pattern around $2\theta = 68°$. It is found that the (242) reflection from the orthorhombic phase is observed between the $(20\bar{2})$ and (422) reflections from the rhombohedral phase at 535 K. This indicates the coexistence of high- and low-temperature phases, which is consistent with the first-order nature of phase transition. This structural phase transition was also observed in the quenched sample.

The open and solid circles in Figure 4(a) represent a_p of quenched and slowly cooled samples, respectively ($a_p = \sqrt[3]{V_O/4}$ or $a_p = \sqrt[3]{V_R/2}$, where V_O and V_R are unit cell volumes of orthorhombic and rhombohedral phases.) The a_p of the quenched sample is smaller than that of the slowly cooled one at each temperature. It seems that the a_p discontinuously decreases with increasing temperature above the transition temperature. The same discontinuous decrease has also been reported at *Pnma*-to-$R\bar{3}c$ phase transition in $LaGaO_3$,[11,12] $LaCrO_3$,[13] and

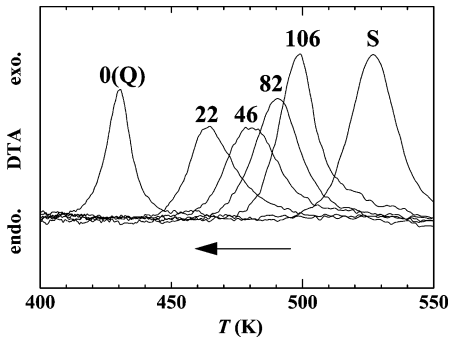

Figure 5. DTA curves on cooling processes. Numerals near each curve indicate the total annealing time in hours at 1337 K before the measurement. Q and S indicate the results of quenched and slowly cooled samples, respectively.

$LaCr_{1-x}Mn_xO_3$.[14] All lattice parameters of the quenched sample shown in Figure 4(b) and (c) are smaller than those of the slowly cooled one, but seem to approach each other with increasing temperature.

Structural Relaxation at High Temperatures. The following experiments were carried out to estimate the relaxation time of relaxation phenomenon around 1300 K. The quenched sample was heated to T_a and annealed there for a certain time in the DTA furnace, and then the sample was rapidly cooled to 673 K and DTA was carried out on cooling at 10 $Kmin^{-1}$ from 673 to 373 K. Successively, the sample was again heated to T_a and the same experiment was repeated several times. Figure 5 shows the total annealing time (t_a) dependence of DTA curve when $T_a = 1337$ K. The numeral near each curve indicates t_a in a unit of hours. Only an exothermic peak was observed in each measurement. The exothermic peak temperature, T_p, shifted to the high-temperature side as the total annealing time increased. If the relaxation phenomenon at 1337 K were due to a first-order phase transition (with the transition temperature above 1337 K) from a supercooled high-temperature phase to a low-temperature phase, two exothermic peaks should be observed based on the orthorhombic-to-rhombohedral phase transitions occurring in the supercooled high- and transformed low-temperature phases. It is thus concluded that the relaxation phenomenon is not due to a certain first-order phase transition. Figure 6 shows the $t_a - T_p$ plot. It is found that T_p tends to saturate to a certain value. Neither appreciable mass gain nor reduction was observed during the experiments, and the XRD after the series of experiments clarified no inclusion of impurity phase. Therefore, it is concluded that the relaxation phenomenon is not due to either reduction of oxygen atoms from the sample nor a chemical decomposition but to a certain structural change in a single phase. The solid line in Figure 6 is the curve obtained by least-squares fitting of the $t_a - T_p$ data with a simple exponential function

$$T_p(t_a) = T_p(\infty) + \{T_p(0) - T_p(\infty)\}\exp(-t_a/\tau) \quad (1)$$

(11) Wang, Y.; Liu, X.; Yao, G.-D.; Liebermann, R. C.; Dudley, M. *Mater. Sci. Eng. A* **1991**, *132*, 13.

(12) Kobayashi, J.; Tazoh, Y.; Sasaura, M.; Miyazawa, S. *J. Mater. Res.* **1991**, *6*, 97.

(13) Oikawa, K.; Kamiyama, T.; Hashimoto, T.; Shimojyo, Y.; Morii, Y. *J. Solid State Chem.* **2000**, *154*, 524.

(14) Howard, S. A.; Yau, J.-K.; Anderson, H. U. *J. Am. Ceram. Soc.* **1991**, *75*, 1685.

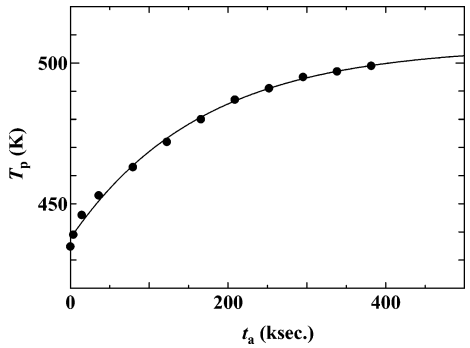

Figure 6. Total annealing time dependence of the exothermic peak temperature of DTA curves indicated in Figure 4. Solid line is the result of least-squares fitting with eq 1.

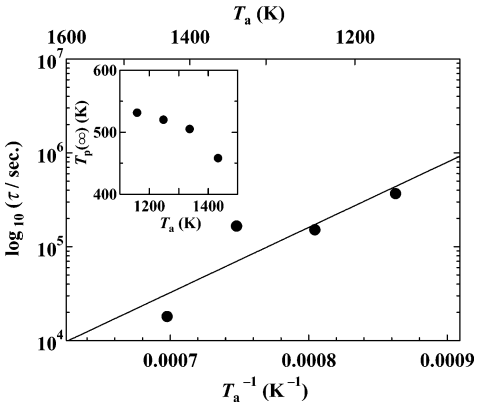

Figure 7. Arrhenius plot of relaxation times obtained by DTA measurements. Solid line is the result of least-squares fitting with eq 2. Inset shows T_p (∞) in eq 1 estimated by the fitting.

The best fit parameters were $\tau = 1.66 \times 10^5$ s, $T_p(0) =$ 438 K, and $T_p(\infty) = 505$ K.

The same experiments were carried out at $T_a = 1443$, 1337, 1243, and 1159 K in the order of decreasing temperature after the sample had almost reached the equilibrium state at each temperature. Figure 7 shows the Arrhenius plot of relaxation times. The solid line in the figure is the result of least-squares fitting with

$$\tau = \tau_0 \exp(\Delta E / R T_a) \qquad (2)$$

The best fit parameters were $\tau_0 = 0.45$ s and $\Delta E = 130$ kJ mol^{-1}. The inset of Figure 7 shows the plot of $T_p(\infty)$ in eq 1 at each T_a. It was found that $T_p(\infty)$ increases as T_a decreases.

Magnetic Susceptibilities at High Temperatures. The open and solid circles in Figure 8 represent the reciprocal magnetic susceptibility of quenched and slowly cooled samples, respectively. The diamagnetic contributions from the closed shell electrons were already subtracted from the raw data. According to the literature,[20] the contribution is -66.5×10^{-6} and -66.05×10^{-6} emumol^{-1} in the case of $LaMn^{3+}_{0.5}Co^{3+}_{0.5}O_3$ and $LaMn^{4+}_{0.5}Co^{2+}_{0.5}O_3$, respectively. The latter value was used for both samples, because the accurate valence distribution of the present samples is unclear and the difference in the diamagnetic contribution due to the difference in the valence distribution is small. The solid lines in the figure are the results of least-squares fitting of the data above 700 K with the Curie−Weiss equation

$$\chi = \frac{C}{T - \theta}. \qquad (3)$$

The best fit parameters were $C = 2.40$ emumol^{-1}K and $\theta = 211$ K for the quenched sample and $C = 2.15$ emumol^{-1}K and $\theta = 322$ K for the slowly cooled sample. A clear anomaly was observed at the orthorhombic-to-rhombohedral phase transition temperature in both samples, as indicated by arrows in Figure 8.

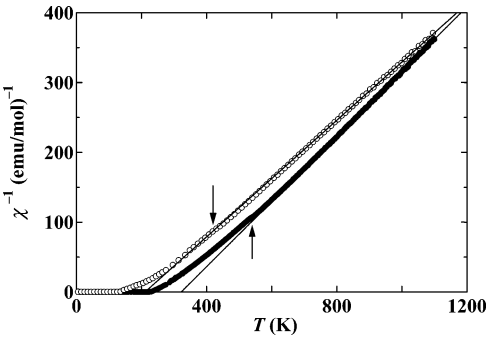

Figure 8. Reciprocal magnetic susceptibility: (●), slowly cooled sample; (○), quenched sample. Solid lines indicate the results of least-squares fitting with eq 3. Arrows indicate anomalies due to the orthorhombic-to-rhombohedral phase transition.

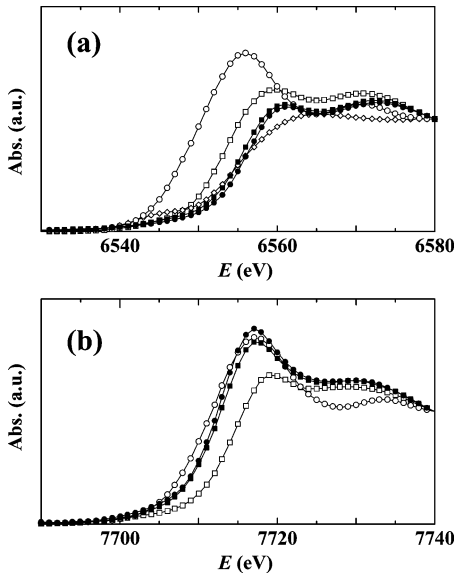

Figure 9. (a) Mn-*K* edge XANES: (●), slowly cooled $LaMn_{0.5}Co_{0.5}O_3$; (■), quenched $LaMn_{0.5}Co_{0.5}O_3$; (○), MnO; (□), $LaMnO_3$; (◇), MnO_2. (b) Co-*K* edge XANES: (●), slowly cooled $LaMn_{0.5}Co_{0.5}O_3$; (■), quenched $LaMn_{0.5}Co_{0.5}O_3$; (○), CoO; (□), $LaCoO_3$.

Mn-*K* Edge and Co-*K* Edge XANES at Room Temperature. The Mn-*K* edge XANES of quenched and slowly cooled samples are shown in Figure 9(a) in addition to those of MnO, $LaMnO_3$, and MnO_2 for the references of divalent, trivalent, and tetravalent Mn atoms. These spectra are normalized at 6530 and 6580

(15) Croft, M.; Sills, D.; Greenblatt, M.; Lee, C.; Cheong, S.-W.; Ramanujachary, K. V.; Tran, D. *Phys. Rev. B* **1997**, *55*, 8726.
(16) Shannon, R. D. *Acta Crystallgr. A* **1976**, *32*, 751.
(17) Inaba, H.; Hayashi, H.; Suzuki, M. *Solid State Ionics* **2001**, *144*, 99.
(18) Himmel, L.; Birchenall, E.; Mehl, R. F. *Trans. AIME* **1953**, *197*, 827.
(19) Hoshino, K.; Peterson, N. L. *J. Phys. Chem. Solids* **1984**, *45*, 963.
(20) Landolt-Börnstein Numerical Data and Functional Relationships in Science and Technology, New Series, Group II, Volume 11; Hellwege, K. H., Ed.; Springer-Verlag: Berlin, 1981.

eV. Both absorption edges of quenched and slowly cooled $LaMn_{0.5}Co_{0.5}O_3$ are higher in energy than those of $LaMnO_3$ and MnO. The spectra of MnO_2 crosses with that of the slowly cooled sample around 6556 eV and that of the quenched sample around 6554 eV. According to the literature,[15] XANES of $CaMnO_3$ also crosses with that of MnO_2 around 6557 eV. Therefore, the absorption edges of quenched and slowly cooled samples are close to that of $CaMnO_3$, and the valence of Mn atoms in $LaMn_{0.5}Co_{0.5}O_3$ is concluded to be nearly tetravalent. However, it is clear that the absorption edge of the quenched sample is lower in energy than that of the slowly cooled one.

The Co-*K* edge XANES of quenched and slowly cooled samples are shown in Figure 9(b) in addition to those of CoO and $LaCoO_3$ for the references of divalent and trivalent Co atoms. These spectra are normalized at 7690 and 7740 eV. Absorption edges of both quenched and slowly cooled $LaMn_{0.5}Co_{0.5}O_3$ are between those of $LaCoO_3$ and CoO. This may be related to the oxidation of Co atoms due to the excess oxygen atoms present in the sample. Despite this, it is clear that the absorption edges of $LaMn_{0.5}Co_{0.5}O_3$ are rather far from that of $LaCoO_3$. The valences of Co atoms in $LaMn_{0.5}Co_{0.5}O_3$ are thus supposed to be close to divalent. It seems that the absorption edge of the quenched sample is higher than that of the slowly cooled one.

Discussion

The equilibrium orthorhombic-to-rhombohedral phase transition temperature, $T_p(\infty)$ in eq 1, increased as the annealing temperature was decreased (see the inset of Figure 7). This indicates that the equilibrium crystal structure depends on temperature even around 1300 K. This is not inconsistent with the earlier reports[3−6] that the relaxation phenomenon is due to slow Mn/Co atomic ordering, because the order parameter increases with decreasing temperature, as indicated by Figure 1. The order−disorder phase transition would occur around 1400 K, because $T_p(\infty)$ seems to change abruptly between 1443 and 1337 K. This is also supported by the magnetic properties described in the forthcoming Part II paper.[10] (No appreciable anomaly was detected in DTA curve around 1400 K possibly because of the second-order nature and/or long relaxation time of Mn/Co atomic ordering.)

The Curie constant of the quenched sample was larger than that of slowly cooled one. This is the same result as that of Jonker.[4] Jonker suggested that the difference in the Curie constant is due to the fraction of Mn^{3+}/Co^{3+} ions in the quenched sample larger than that in the slowly cooled sample, because the theoretical Curie constants are 1.88 and 3.00 emumol^{-1} K for 50:50 Mn^{4+}/Co^{2+} and 50:50 Mn^{3+}/Co^{3+}, respectively, when only spin contribution is considered. This suggestion is consistent with the following results presented as (1)−(5). (1) XANES clarified that both Mn-*K* and Co-*K* edges of quenched sample shifted to their trivalent state side from those of the slowly cooled one. (2) The a_p of the quenched sample was smaller than that of the slowly cooled one. This is consistent, because the average size of B(Mn/Co) site ions is 0.63 Å for 50:50 Mn^{3+}/Co^{3+} and 0.64 Å for Mn^{4+}/Co^{2+} according to Shannon's ion radius.[16] (3) The α_R of the quenched sample was smaller than that of the slowly cooled one. This is understood by a well-known torelance factor, $t = d_{La-O}/\sqrt{2}d_{B-O}$, where d_{La-O} and d_{B-O} are equilibrium bond lengths between La and O atoms and between B and O atoms. The tolerance factor, 0.957, is less than unity when B = 50:50 Mn^{4+}/Co^{2+}. The replacement of some Mn^{4+}/Co^{2+} by Mn^{3+}/Co^{3+} decreases d_{B-O} and lets t approach unity. The tolerance factor of the quenched sample being closer to unity decreases the tilt angle of BO_6 octahedra and thus α_R from those of the slowly cooled sample. (4) The rhombohedral-to-orthorhombic phase transition temperature in the quenched sample was lower than that of the slowly cooled one. This would be due to the tolerance factor being closer to unity.[17] (5) The a_p of the quenched sample was smaller than that of slowly cooled one even at 30 K. This implies that Mn^{3+}/Co^{3+} ions exist even at 0 K in the quenched sample due to the disordered Mn/Co atomic configuration.

The unit cell volumes of slowly cooled and quenched samples approach each other with increasing temperature, though the diffusion rate of Mn/Co atoms is very small there according to eq 2. This suggests that the fraction of Mn^{3+}/Co^{3+} increases with increasing temperature even in the slowly cooled sample, namely thermally equilibrium reaction occurs between Mn^{3+}/Co^{3+} and Mn^{4+}/Co^{2+} valence states at the temperature region.

The activation energy of the relaxation time is close to those (100−200 kJ mol^{-1}) of diffusion constant of Fe atoms in $Fe_{1-\delta}O$ with $\delta \approx 0.1$[18] and divalent, trivalent, and tetravalent transition-metal ions in $Co_{1-\delta}O$ with $\delta \approx 0.01$.[19,21] Though the Mn/Co atomic ordering is not a simple diffusion process, the relaxation time of ordering should be connected with the diffusion constant. Therefore, the magnitude of activation energy implies that the relaxation is connected with the diffusion of Mn and Co atoms. The activation energy of diffusion constant based on a vacancy mechanism is generally the sum of activation energies of migration and vacancy formation.[22] However, the activation energy, 124 kJ mol^{-1}, of diffusion constant of Fe atoms in $Fe_{1-\delta}O$ includes only the migration component, because $Fe_{1-\delta}O$ has much intrinsic vacancy at the Fe site.[18] $LaMn_{0.5}Co_{0.5}O_{3+\delta}$ might be the same case as $Fe_{1-\delta}O$, because the relatively large excess oxygen nonstoichiometry, $\delta = 0.03-0.04$, indicates the presence of many vacancies at the Mn/Co site (and La site).

Conclusions

The present results are consistent with the conclusion of earlier studies[3−6] that the Mn/Co atomic ordering freezes-in around 1300 K due to enlarging the relaxation time, that the ground valence state is Mn^{4+}/Co^{2+}, and that the Mn^{3+}/Co^{3+} state is mixed by disordering the Mn/Co atomic configuration.[3−6] In addition, the present results suggest that the Mn/Co atomic ordering proceeds through a second-order phase transition and that the Mn^{3+}/Co^{3+} state thermally equilibrates with the $Mn^{4+}/$

(21) Nowotny, J.; Sadowski, A. *NATO ASI Ser., Ser. B* **1985**, *129*, 227.
(22) Shewmon, P. G. *Diffusion in Solids*; McGraw-Hill: New York, 1963.

Co^{2+} state at high temperatures. This implies that the Mn/Co atomic ordering occurs even in the presence of charge fluctuation between Mn^{4+}/Co^{2+} and Mn^{3+}/Co^{3+}. In the forthcoming Part II paper, we report the correlation between magnetic properties below room temperature and Mn/Co atomic order.[10]

Acknowledgment. Part of this work was financially supported by a Grant-in-Aid for Scientific Research from the Ministry of Education, Science, Culture, and Sports of Japan.

CM0302781